Available online at www.sciencedirect.com

ScienceDirect

Energy Procedia 63 (2014) 4339 – 4357

Energy Procedia

GHGT-12

Analysis of the passive seismic monitoring performance at the Rousse CO_2 storage demonstration pilot

Xavier Payre[a]* - Christophe Maisons[b] - André Marblé[a] – Sylvain Thibeau[a]

[a]*TOTAL Exploration & Production, 64018 Pau Cedex, France*
[b]*Magnitude, Centre Regain, 04220 Sainte-Tulle, France*

Abstract

In January 2010, an integrated CO_2 Capture and Storage (CCS) project, including CO_2 capture, transportation and geological storage started in the Lacq-Rousse area, Southwest of France. Until March 2013, 51 thousands metric tons of CO_2 were injected into a fractured dolomitic depleted gas reservoir at around 4500-m depth. Key objectives of the project were to develop, test, and validate the methodology and the technology required for managing safely such storage operations, and in particular to define an "optimal" monitoring program, economically and technically viable.

A monitoring plan was designed, including the deployment of a hybrid multi-scale passive seismic monitoring network to address 3 monitoring objectives: watch seal integrity, distinguish natural seismicity from induced seismicity, and assess injection-induced seismicity. A near-surface network (Master Network), and a downhole array deployed in the injection well (Research Network), were installed between 2009 and 2011. In addition, detection of regional seismicity was also available through a seismometer.

Data have been collected for 9 months prior to injection, during injection, and also after injection, as part of the post-injection monitoring program planned for 3 years. Starting from March 2011, as per end July 2014, the hybrid system allowed detecting about 2500 events. Over two third of those events were not energetic enough to be located. Over 600 events, with estimated magnitudes above -2.3 and not exceeding -0.5 were located in the reservoir. The monitoring therefore helped in concluding that the CO_2 injection did not generate an adverse impact on reservoir integrity. Actual network performances have been in line with expectations. The effective Master Network location sensitivity is about magnitude -0.6 (completeness magnitude) in the volume of interest, confirming its ability to serve for an efficient seismic hazard monitoring.

* Corresponding author. *E-mail address:* xavier.payre@total.com

Peer-review under responsibility of the Organizing Committee of GHGT-12
doi:10.1016/j.egypro.2014.11.469

In this paper we show how the proper design of a passive seismic network consistent with the monitoring plan can benefit the different phases of a CCS project, and how passive seismic monitoring during the full duration of the injection can bring reliable evidence for reservoir integrity. The paper concludes that passive seismic monitoring with a limited number of near-surface sensors constitutes an effective alarm network. In addition passive seismic monitoring can provide a permanent seismic risk evaluation tool by continuously comparing seismic activity with the energy input into the reservoir. This second type of application is certainly not necessary for most oil and gas development, but it may constitute a precise element of monitoring if seismic hazards need to be closely monitored.

Peer-review under responsibility of the Organizing Committee of GHGT-12

Keywords: CCS; passive seismic monitoring; multiscale hybrid network; nanoseismicity; McGarr equation

1. Introduction - Qualifying an integrated CCS chain

In 2007, Total announced the launch of an end-to-end CO_2 capture, transportation and storage pilot at the Lacq basin, in Southwest France (Fig. 1). Carbon dioxide, produced by industrial facilities in Lacq, was to be captured, transported through a 27-km long pipeline, and injected in a gas phase, at a limited rate, over 2 years, in a 4,500-m deep depleted gas reservoir, the Mano reservoir, in the Rousse field.

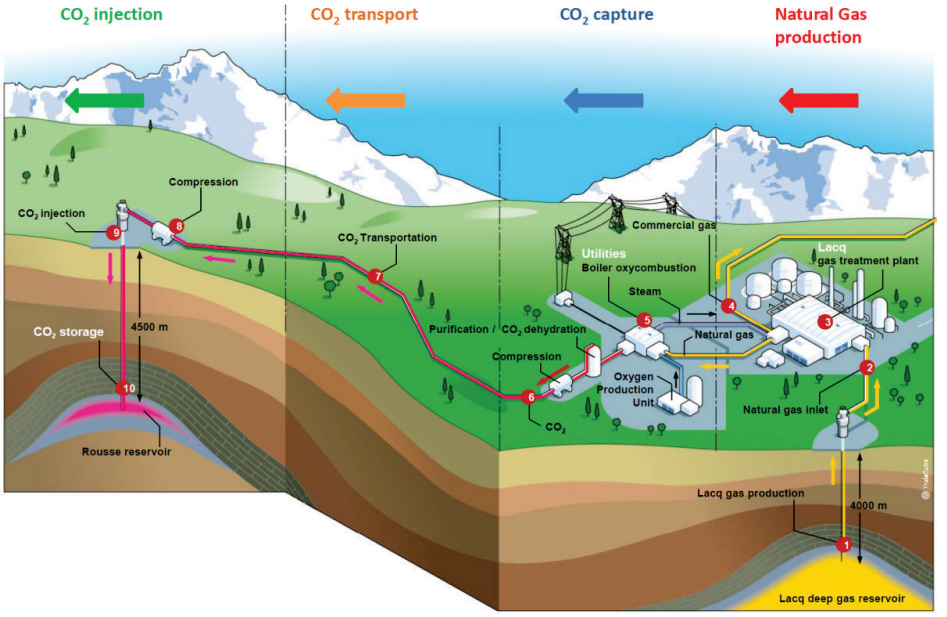

Fig. 1 - The Lacq-Rousse integrated CCS chain.

One objective of the Lacq CO_2 Capture and Storage (CCS) project was to demonstrate the technical feasibility and reliability of an integrated onshore industrial CCS chain. Another aim was to identify, apply, and validate geological storage qualification methodologies, monitoring and verification techniques on a real operational case to be able to develop at optimal cost larger-scale CCS projects.

In January 2010, the first complete industrial scale CCS chain in Europe was up and running. Over the following three years, more than 51,000 metric tons of CO_2 were successfully injected into the fractured dolomitic Mano reservoir. Injection rate into the reservoir was 70 tons-per-day on average.

The Rousse depleted field is a deep isolated Jurassic horst located to the north of the North Pyrenean Thrust Front and to the south of Meillon Saint-Faust fields (Fig. 4). It was structured during the north-east extension phase of the pre-Pyrenean rifting [1].

The Lacq-Rousse demonstration CCS Pilot corresponds to an increase of Mano reservoir pressure from 42 bars to 85 bars, far below the initial reservoir pressure of 485 bars. The risk of a potential CO_2 leakage is extremely low. Nevertheless the monitoring program deployed at Rousse on the basis of the Total qualification studies and French Administration requirements is very complete as the project provided a good opportunity to test new monitoring tools.

An extensive surveillance program was designed accounting for all identified possible hazards, including potential risks of leakage via an undetected fault or a crack in the injection well. The monitoring plan, containing quantitative threshold values, was submitted to, and subsequently approved by, the regional Industry, Research and Environment Board (DREAL), at the end of 2008, 15 months before the beginning of the CO_2 injection [2].

Among the monitoring methods available to identify the effects of the injection on the reservoir and on the caprock, “passive seismic surveillance” appeared as an essential component of an early warning system. The aim of the passive seismic component of the monitoring system was to verify that injection operations were having no mechanical impact within and outside the reservoir, and to distinguish between induced seismicity in pilot area from naturally tectonically active surroundings.

These operations have been monitored with a hybrid multi-scale passive seismic network comprising a near-surface network (Master Network), and a downhole array deployed in the injection well (Research Network) installed between 2009 and 2011. Seven 200-m deep wells with vertical seismic arrays and a surface seismometer formed the Master Network whose role was to carry out “Seismic Hazard Monitoring”. In addition, the injection well was equipped with an “R&D” deep downhole array. Seismic data started to be collected 9 months prior to injection, and a post-injection monitoring is still ongoing [3].

This paper presents the design of the passive seismic network, and discusses some of the passive seismic monitoring results, including the analysis of its performance, and its suitability for achieving the goals set up for its design. It shows how microseismic technology can benefit the different phases of a CCS project, from feasibility phase (“how to design a microseismic network consistent with the monitoring plan?”) to operational phase (“how can microseismic monitoring during the duration of the injection bring reliable evidence for reservoir integrity?”). The paper will conclude with our current thinking about lessons learnt, and benefits of those technologies.

2. Natural, Induced and Triggered Seismicity - Nanoseismicity

2.1. Natural vs. Anthropogenic Seismicity

Earthquake activity in the Earth's crust is known as seismicity. Natural earthquakes are often viewed as unpredictable phenomena caused by naturally shifting stresses in Earth's crust. Change in stress increases or decreases strain, which weakens the stability of faults confined by the stress. Faults may then slip and release repressed energy, which then propagates as elastic waves through the geological media. With a proper monitoring system, earthquake parameters such as epicenter, depth, occurrence time and strength may be estimated. The source mechanism, the size and the type of rupture may additionally be known.

In reality, however, “artificial” anthropogenic earthquakes are observed. A range of human activity may affect stress, pore pressure, strain, fluid saturation, fluid flow and rock strength in the subsurface, and induce earthquakes. When caused by, or possibly linked to, a human activity that alters the stresses and strains on the Earth's crust, seismicity is commonly referred to as "**induced seismicity**." Industrial activities that have been associated with induced seismicity include impoundment of large reservoirs, mining, oil and gas production, geothermal energy production, construction, underground nuclear testing...

Induced stresses can range from a few tens of kPa, to several MPa. Induced seismicity refers to typically minor earthquakes and tremors that are of relatively low magnitudes. Nearly all instances of induced seismicity are not felt on the surface and do not cause damage. Felt earthquakes associated with any oil and gas production activities are rare.

The causes and mechanics of earthquakes caused by human activity and the means to decrease their associated risk are not fully understood yet. A discontinuity may be weakened and reactivated if pore pressure is increased or by changing the shear and normal stress acting on it (Fig. 2). When injecting or producing a fluid, the mechanism responsible for inducing seismicity at any scale appears to be changes in volume and pore pressure that alters the effective stress within a reservoir and its surroundings. These changes may reactivate a preexisting fault (triggered seismicity), or induce new ruptures (induced seismicity). These stress changes can result in a variety of focal mechanisms.

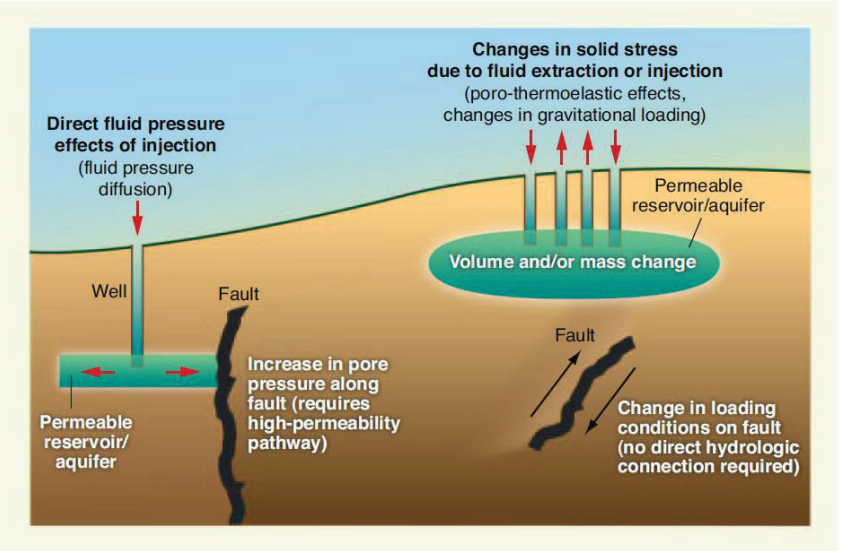

Fig. 2 - Mechanisms for inducing, triggering Earthquakes
Schematic diagram of potential causative mechanisms for triggered/induced earthquakes
(after B. Ellsworth 2013 - [4])

2.2. Microseismicity and nanoseismicity

The “rupture phenomena”, including earthquakes, are observed from microscopic to macroscopic scale. Seismic events too small to be felt on the surface are known as microearthquakes. In seismology, the term “microearthquake” traditionally refers to seismic event with magnitude lower than 3 (however for some authors the terms refers to seismic events with magnitudes below 2).

As the range of low magnitudes constitutes an open scale, and as small scale ruptures associated with microearthquakes scan from micrometric to hectometric features, we usually tend to favor the more precise classification proposed by Bohnhoff [5]. The following table (Table 1) provides a general overview of monitoring domains based on the magnitudes and proposes an appropriate classification of seismic events for hazard assessement and reservoir characterization.

In the case of CCS monitoring, most detected events should be thousand times weaker than those named microseisms in seismology: we expect to record mostly nanoseismic events with magnitudes greater than -2 but lower than 0, and even, with a suitable network, some picoseismic events (between magnitude -4 and -2).

Table 1 - Passive seismic domains.
Values for rupture size for the microearthquake range, adapted to the specificities of Rousse CCS (ref. to hypotheses) presented below the main table *(after Bohnhoff et al., ILP, 2010 [5]).*

Passive Seismic Domains & Magnitude Ranges

After Bohnhoff et al., ILP's Second Potsdam Conference, 6-8 Oct. 2010

Domain	Magnitude Range	Event Class	Fault Size	Displacement Scale	Event Type
Seismology "Seismic Hazard"	8 or more	Great	100 - 1000 km	4-40 m	Earthquake
	6 to 8	Large	10 - 100 km	0.4-4 m	
	4 to 6	Moderate	1 - 10 km	40-400 mm	
	2 to 4	Small	0.1 - 1 km	4-40 mm	
Induced seismicity monitoring	0 to 2	Micro	10 - 100 m	0.4-4 mm	Microearthquake
	-2 to 0	Nano	1 - 10 m	40-400 µm	
	-4 to -2	Pico	0.1 - 1 m	4-40 µm	
Lab Test	-6 to -4	Femto	1 - 10 cm	0.4-4 µm	Acoustic Emission
	-8 to -6	Atto	1 - 10 mm	40-400 nm	

Approximate length and displacement for stress drops of 3 MPa

Reservoir surveillance

Fracture characterization

The Rousse CCS case study

Induced seismicity monitoring	0 to 2	Micro	10 - 200 m	50 µm - 3 mm	Microearthquake
	-2 to 0	Nano	1 - 20 m	5-300 µm	
	-4 to -2	Pico	0.1 - 2 m	0.5-30 µm	

Hypotheses Circular fault Stress drop: 0.1-1 MPa Shear modulus: 25-30 GPa

Triggered vs. Induced Seismicity – Associated magnitudes

The term "induced seismicity" is often used to refer to any seismic event linked to (i.e. caused by, or influenced by) human activity: triggering and/or driving of the rupture is controlled by human-made stress or pressure perturbations. Some researchers, however, more narrowly define "induced seismicity" activity with the introduction of two categories [6]. Because the amount of influence a human activity has on a seismic event is hard to establish, the distinction is not always made.

Indeed, when stimulating a geologic medium through injection or production, two types of seismic events may occur, each with specific characteristics in terms of energy level, time frame, location, and scale:

- **Induced nanoseismic events,** as an inherent part of the process: the rupture is driven by the human-related (induced) stress or pressure perturbation. The earthquake would not occur without the human operation. Induced events are very small events: they are nanoseismic, picoseismic, and weaker, and therefore can genuinely be considered as minor. They are observed in the vicinity of the stimulation during the stimulation period. They do not create harmful effects and require very sensitive monitoring equipment to be detected. Such events caused solely by human activity, are considered as means to understand the reservoir stimulated volume and/or the shear-enhanced permeability.
- **Triggered microseismic events**, as the result of fluids or pressure interacting with existing geological faults. Triggered earthquakes are larger events than induced microearthquakes: these are usually microseismic events. They create more significant failures and mass accelerations, potentially felt, in rare circumstances, by humans at the ground surface (true “seismic” events). They may be observed at a larger distance from stimulated zone, during and after the stimulation period. When describing an event as triggered, this indicates that the stress was accumulated through natural processes, but the mechanism that caused the stress release was an effect of human activities. The occurrence of a triggered event is advanced in comparison to the background rate, but the size of the event is controlled by the existing natural stress field and rupture structure. These unintended events can be avoided through site selection, injection design and permanent monitoring.

Distinguishing between triggered and induced earthquakes becomes important if the seismic hazard and earthquake size is questioned.

3. Seismic hazard monitoring objectives - Design criteria

3.1. Expected features of seismic activity

There are several published case studies of significant seismicity caused by operations involving a change in volume (removal of a volume of matter when extracting a solid rock, or producing a fluid, or addition of a volume when injecting a fluid volume). These activities produce shear stresses released by microearthquakes that can in particular damage a borehole by offseting faults. They can also adversely affect public opinion: unexpected high levels of the seismic activity have lead to the stand-by or termination of some projects.

The basic parameters commonly used to report and characterize the level of induced seismicity are:

- the number of events detected and the number of events located,
- the scalar seismic moment $M_0 = \mu.A.d$ (μ: shear modulus - A: area of slip - d: displacement of slip),
- and the moment magnitude $M_W = 2/3 \log(M_0) - 6.07$ (where M_0 is in N.m or J).

The Earthquake scaling diagram presented in Figure 3 shows the scaling relationship between rupture sizes (fault size and slip amplitude), deformation (seismic moment and stress drop) and the moment magnitude (a pseudo "Richter scale" commonly used for simplicity). An objective parameter for measuring the level of seismicity is certainly the total released seismic moment. It can be defined as the scalar sum of seismic moments and is proportional to the released energy.

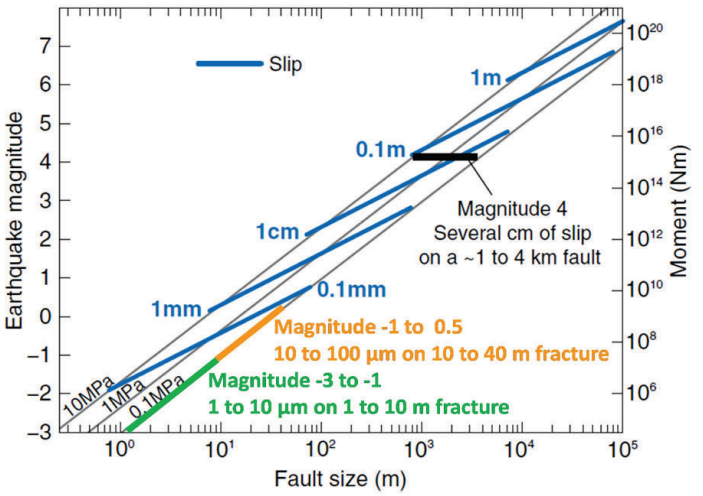

Fig. 3 - Earthquake scaling diagram *(modified after Zoback, and Gorelick 2012 [7])*
Relationship among various scaling parameters for earthquakes.
The larger the earthquake, the larger the fault and amount of slip, depending on the stress drop.
Observational data indicate that earthquake stress drops range between 0.1 and 10 MPa.

In a CCS project, even if there are numerous factors influencing the seismic activity, a very simple approach to assess the maximum seismic activity is to consider the seismicity that results from ground deformation to be associated with changes in pressures and stresses originating from the change in volume: as a matter of fact we can consider that the total injected volume of an incompressible fluid must be preserved and could be accommodated only by seismic failure.

McGarr [8] noticed a correlation between the total energy released during rock extraction and the volume of rock extracted. He proposed a model relating total seismic moment resulting from ground deformation to volume change through either extraction or injection. The McGarr equation is a proportional relationship between the total released seismic moment (ΣM_0, in Nm), proportional to the total energy released, and the change of volume (ΔV, in m^3):

$$\Sigma M_0 = K.\mu.|\Delta V|$$

where μ is the shear modulus (in Pa),
and K is a dimensionless factor smaller than, and generally close to, 1.

The McGarr equation provides a means of estimating the amount of seismicity associated with a fluid injection. Most of the injection related projects show significantly lower released seismicity than the McGarr prediction: this is probably caused by significant energy loss by aseismic processes.

As shown by McGarr [9] the model appears to define the magnitude of injection-induced seismicity from few cases of anomalous seismicity during geothermal, waste injection and stimulation operations. Thus the model can be considered as a way to estimate the upper bound for induced seismicity resulting from fluid injection: the total moment can be considered as the moment released by a single event, assuming all input energy being released in this single event. This largest possible seismological event is referred as the seismologic potential.

In the case of the Lacq-Rousse CCS demonstration project. 51 kt CO_2 at 42 to 85 bar downhole pressure and 150°C temperature correspond to an in-situ injected volume of about half a million cubic meters and, according to McGarr equation assuming 100% effectiveness, to a seismologic potential of about magnitude +4.7. This value can be considered high, but one should not forget:

- The equation used for the computation is originally based on the observation of a rock removal (mining) process and is being applied to a compressible fluid injection;
- The estimate corresponds to an upper bound of energy that cannot be released in a single event. Indeed according to Gutenberg-Richter distribution law, many smaller events should be observed: the largest observed event would actually have a lower magnitude, depending on b-value. We would expect induced seismicity, meaning a high b-value and thus a small percentage of total seismic energy released in the largest event.
- Most importantly, the Mano reservoir, capped by a layer of clay and marl 2,000 m thick, is highly depleted. It has contained gas for millions of years at a pressure much higher (initial pressure: 485 bar) than the pressure that will be reached at the end of the injection operations and has withstood the powerful seismic tremors that occurred in the Tertiary period before the Pyrenees were formed. The volume change (~500,000 m^3) and the pressure change (from 42 to 85 bar) are very small compared to the volume of gas produced (3.3 Mrm^3). No large event occurred during the depletion. The probability for an event of "large" magnitude to occur in Rousse due to reinjection is negligible. Finally the geomechanical modeling performed during the design study did not predict brittle failure and/or reactivation of the major faults [10].

In conclusion, the energy released as seismic energy is expected to be very low compared to McGarr prediction. The effective ratio $\Sigma M_0 / |\Delta V|$ will provide a good indicator to characterize the level of seismic deformation with respect to the maximum theoretical ratio predicted by the McGarr equation.

3.2. Passive seismic monitoring objectives & Design Criteria: a three-scale network

When building the program for the Lacq-Rousse CCS demonstration pilot, general expectations set up to design the passive seismic monitoring network at Rousse were defined at two levels:

- The first priority is to carry out the surveillance of the injection and storage operations.
- The second objective, for research purposes, is the acquisition of data to analyze the nanoseismicity expected to occur within the reservoir.

Primary objective: seismic hazard monitoring. This primary objective encompasses two aspects:

- The surveillance of the seal integrity i.e. the identification of any mechanical effects that could affect the integrity of the storage during and after the injection period. Considering the seismologic context of the reservoir, this infers setting up an alarm in case of high magnitude regional earthquake (larger than magnitude 3). Should alarm be occurring during injection, then injection operations could be stopped.
- The implementation of a seismic monitoring component that would confirm that the storage behaves as predicted, with the ability to detect any seal failure and CO_2 migration to shallower formations through unidentified subseismic faults or fractures.

Secondary objective, research: assessing "injectivity". The objective is to assess the CO_2 plume extension and to characterize the dynamic behavior of the reservoir (correlations between injection rate, cumulative volume injected and rate of seismicity) by analyzing the nanoseismicity distribution along with the injection parameters, assuming a direct causal relationship. This objective requires a more sensitive monitoring of the injection to access detailed information on the reservoir behavior:

- Detection of nanoseismic, and possibly picoseismic, events in the vicinity of the CO_2 injection well.
- Estimation of pressure perturbation and fluid front migration.

To account for both objectives, three scales, i.e. ranges, and consequently corresponding components (sub-networks), have been considered to properly define the passive seismic monitoring network: the regional scale, the field scale, and the reservoir scale. The quantitative targets considered for each sub-network are set more severe than those requested by regulations to design the network.

3.3. Network component for Seismic Hazard Monitoring: Passive seismic surveillance of seal integrity

The first main objective of Rousse CCS seismic surveillance is to monitor any small scale "fault type seismicity" (b-value =1) that might endanger the reservoir seal integrity. This surveillance needs to encompass the rock volume from surface to reservoir within a 5-km radius from injection well (equivalent to injection depth), with a focus on a 1.5-km radius (larger than the CO_2 plume expected extension) (See Fig. 4).

Maximum estimated possible rupture size is about 100 meters with displacement below 1 millimeter, corresponding to a maximum magnitude of less than +2.0 (Table 1). As a consequence the magnitude sensitivity expectation for the system has been set up at about -1 optimally, with the minimum requirement to be better than 0 (magnitude considered as a pre-warning threshold from monitoring perspective).

The operating period for seismic hazard monitoring covers the life of the project. As it is an essential component of the monitoring program, the design needs to account for reliability and redundancy. Optimally recording should start at least half a year before start of injection to allow for recording a meaningful baseline.

3.4. Network component for Public Awareness: Monitoring seismologic context

The Pyrenees are a range of mountains forming the natural border between France and Spain. They stretch in a west-east direction over about 500 km, separating the Iberian Peninsula from the rest of continental Europe. Their width varies between 65 and 150 km. The Pyrenees have experienced a very long geological evolution with multiple orogenies. Since the Eocene the orogeny still undergoes strong erosion, isostatic movements, post-kinematic extension, and even renewed compression that can cause medium-sized earthquakes.

Thus the second main objective of Rousse CCS seismic surveillance system is to account for the specific seismologic context and monitor natural Earthquake activity (b-value = 1) in complement to the National Seismological Network, and thus improve locally the accuracy in the location of hypocenters. This monitoring concerns a regional scale with a radius of about 30-km around the injection well where National Network is reporting small to moderate earthquakes on a regular basis. Faults involved in the rupture are considered to be at the kilometer scale. Most probable events will have a magnitude up to 4. The alert threshold considered is magnitude 2 within Rousse perimeter (5-km radius from injection). So the network sensitivity is expected to be better than 1.5, with a location accuracy of approximately 1 km.

The monitoring period for Public Awareness covers the life of the project.

3.5. Network component for R&D: Observing fracturation process

The secondary objective of Rousse CCS seismic surveillance system reservoir is to monitor and analyze the micro-fracturing swarm type of induced nanoseismicity, the expected by-product of injection, by having a reservoir-scale view, within 1 km from injection. Fracture characterization calls for higher network sensitivity in order to be able to:

- Map small features. Rupture size (fractures) is expected to be much less than 25 m with a 0.2 mm slip, corresponding to a magnitude +0.6 microseismic event.
- Get a more complete catalogue allowing for a good estimate of a- and b-values in Gutenberg-Richter relationship (expected b-value > 1).

As we are interested in studying the swarm of nanoseismicity (magnitude smaller than 0) and possibly picoseismicity (magnitude smaller than -2), the required magnitude sensitivity for the corresponding network component should be better than -1.5, -2.0 being considered optimal to locate enough events. Coverage required needs to be larger than the maximum CO_2 plume extension, thus a requirement for coverage on a 750-m radius from injection points over the reservoir thickness, with location accuracy better than 100 m.

Monitoring period covers at least the entire injection phase. Optimally however, recording should start before the start of injection to allow for recording a meaningful baseline, and continue after the stop of injection until the pre-injection state is recovered.

Considered alert threshold is magnitude 1, over what has been considered to be the largest expected event.

Finally access to parameters relative to the source focal mechanism would add extra value to the R&D component of the passive seismic monitoring project.

3.6. Passive seismic monitoring at Rousse - Design study and selected concept

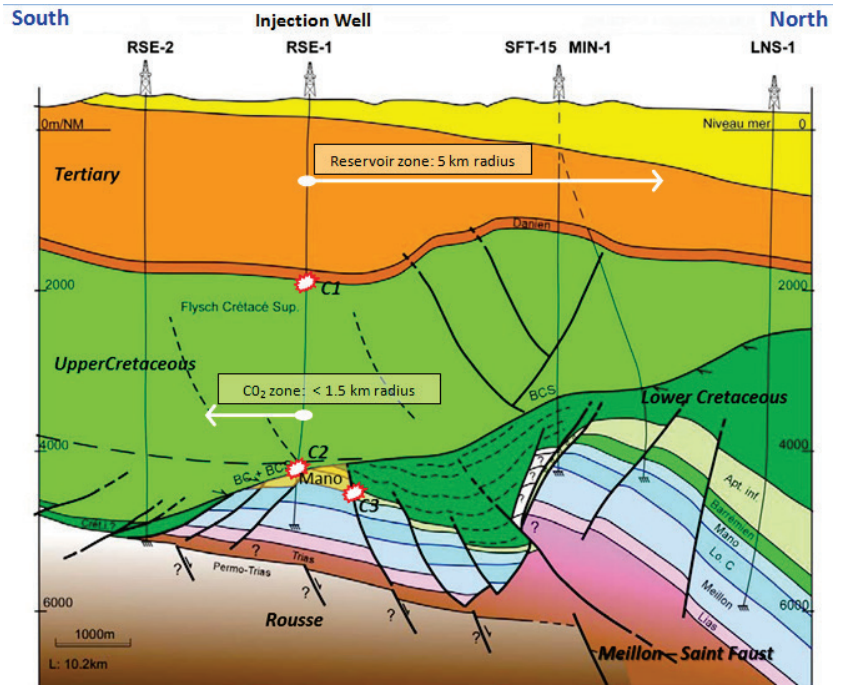

Fig. 4 - Geological environment of the CO_2 storage
Radii of investigation for surveillance.
Three characteristic events have been considered for the network design: Top Danian (C1), Mano reservoir (C2), and a seismic fault (C3)

Design criteria have been described in the previous sections, in terms of zone of interest (i.e. range, both vertical and horizontal), sensitivity, and location accuracy.

The fractured dolomitic Mano reservoir lies at 4545-m below ground level. The three main zones considered for integrity during the microseismic screening, feasibility and modeling phase are the Top Danian seal, the Mano reservoir (induced seismicity), and border faults (Fig. 4).

The comprehensive feasibility study, including screening, design, and modeling, indicated that the coverage and location accuracy required for the main objective of passive seismic surveillance of seal integrity could be provided by a "Master" Subsurface Network. Hypotheses considered in the 2007 study were:

- Background noise: 0.5 µm/s (worst case).
- Calibrated velocity model.
- Explosive source.

A passive seismic monitoring network has been designed and put in place to record any seismic events that might affect the clay and marl caprock overlying the reservoir. The selected ambitious multi-scale hybrid system combines three distinct components aimed at monitoring respectively Triggered Seismicity and Natural Earthquake (Master Network), and Induced seismicity (Research Network).

The resulting estimates of location uncertainties for events of magnitude -1 detected by the Master Network are: C1 ± 100 m; C2 ± 240 m; C3 ± 260 m (Fig. 5).

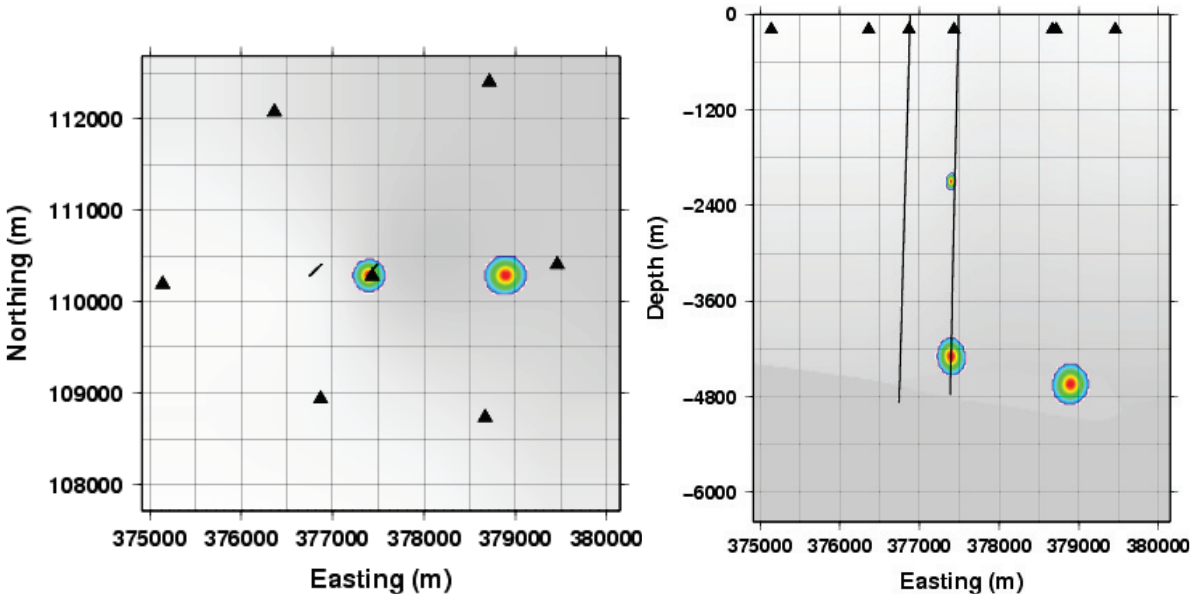

Fig. 5 - Master Subsurface Network - Location uncertainty (probability density function) color coded (a) map view; (b) section view

The **Master Network** aims at achieving hazard identification (triggered seismicity) and public awareness (natural earthquakes) objectives. This "conventional system" comprises 1 surface seismometer, and 7 Shallow-Buried Arrays (SBA's) with an aperture of 2-km around the injection well (Fig. 6). Each SBA consists of a well 200-m deep, fitted with a vertical array of four 10-Hz triaxial-geophones that can record events of a magnitude as low as -1 (corresponding to a slip of a few hundredths of millimeter along a metric fault), within a 1.5-km-radius zone around the injection well, from reservoir to surface. The surface seismometer, moved close to the quietest SBA after a few months, monitors natural seismic activity in the region.

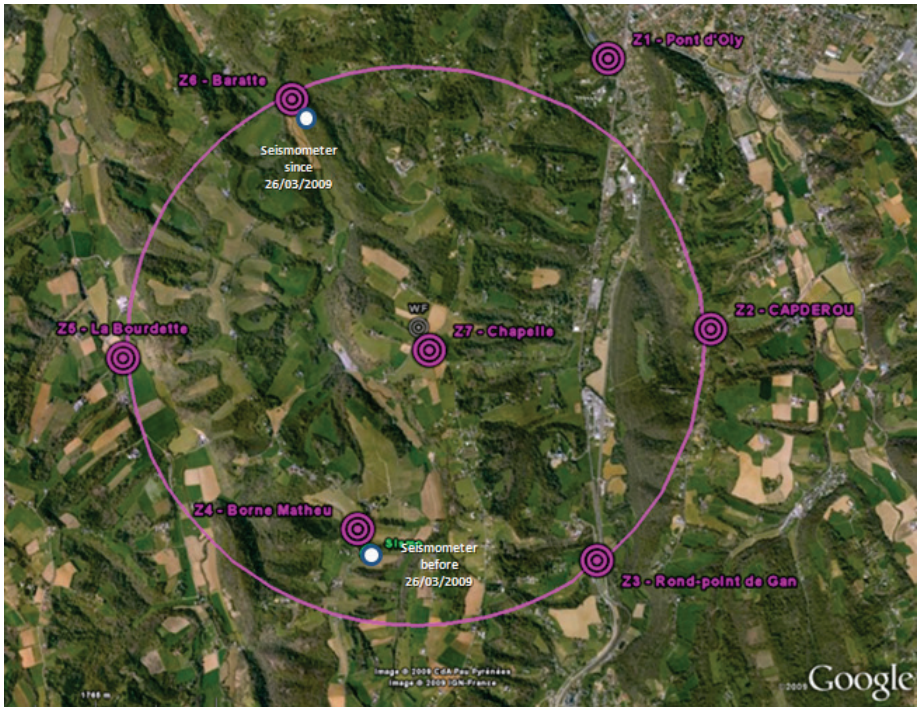

Fig. 6 - Master Network with 2-km aperture. Location of SBAs (purple circles). Station Z7 is close to injection well.

Depths for buried sensors were selected after ambient noise tests, to improve Signal-to-Noise Ratio (SNR). This critical improvement allows achieving required sensitivity with a limited amount of stations. The number of stations and the geometry of the SBA-based network are sufficient to:

- Keep sensitivity and location accuracy within specifications in case of failure.
- Provide adequate spatial sampling to enable proper inversion for source mechanism of high SNR events.

No significant events were recorded within this zone of interest during the three-year injection phase.

The **Research Network** aims at recording all nanoseismicity induced by CO_2 injection. The selected solution, a Downhole Array (DA) installed 4,500 m below the surface within the injection well, may be considered as innovative. It consists in 3 tubing conveyed Fiber Optic triaxial sensors (accelerometers) installed in the injection well, above the Mano reservoir, between 150 and 350 meters above the injection points.

Even considering some increase of the background noise level during injection operations, the system theoretically allows to detect all isotropic nanoseismic events (moment magnitude down to -2) within the zone of interest (750-m radius from injection points). This magnitude corresponds to nanoseismicity that could be associated with a slip of a few micrometers along a sub-metric rupture plane.

We are aware that recording with a single linear array introduce some biases in the experiment, depending on the source location and focal mechanism, and do not allow for accurate moment tensor estimation. Nevertheless the results acquired through the experiment are up to our expectations.

Due to operational incidents, the research system was up and running only in March 2011, after the start of injection. Thus, unfortunately, we have no base line to assess nanoseismic activity prior to the injection.

4. Results & Analysis - Natural seismicity, triggered microseismicity and induced nanoseismicity

4.1. General observations

Data started to be collected starting from nine months prior to injection (only by Master Network), and continued after injection. A post injection monitoring is ongoing including both the Master (7 SBAs and 1 seismometer) and the Research (1 DA) Networks.

From March 2011 to July 2014 the whole system detected 3,770 events (240 quarry blasts, 970 Pyrenean earthquakes), and 2560 reservoir related events).

The general surveillance, performed by the Master Network, identified the activity related to natural seismicity on North Pyrenean faults (970 earthquakes) and very low seismicity (32 events with magnitude ranging from -0.75 to +1.8) on border faults of a nearby gas field. As for activity a priori related to CO_2 injection (induced seismicity), only 4 events with magnitude between -0.7 and -0.3 could be located by the Master Network in the vicinity of the injection well (SBAs detection sensitivity is about -0.8 over the injection zone (Fig. 7).

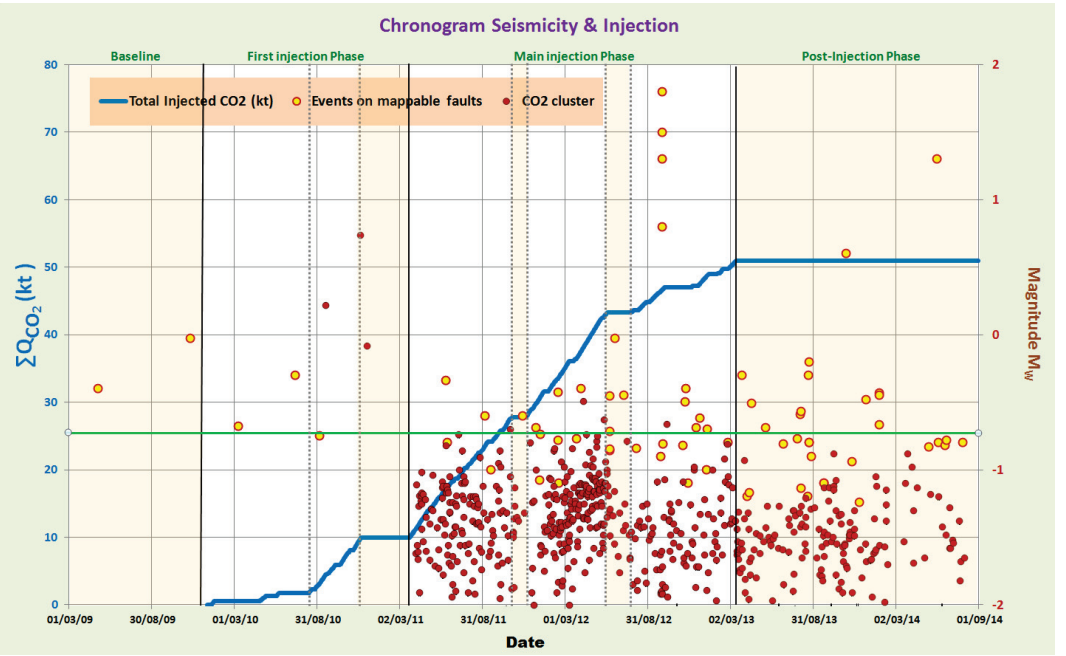

Fig. 7 - Seismicity versus Injection. Data acquisition with Downhole Array started in March 2011
Events are colored by location (see Fig. 8): red dots correspond to events located in the CO_2 zone;
yellow dots are events located along border faults of a northern gas field.
Master Network active during Baseline and First Injection Phase. Effective location sensitivity is about -0.7 over the whole reservoir.
Master & R&D Networks active during Main Injection Phase and Post-Injection Phase.
Location sensitivity better than -2.0 on CO_2 zone and about -0.7 over the reservoir zone

The reservoir detailed monitoring, performed by the Research Network (Downhole Array), identified additional nanoseismicity along border faults (39 events with magnitude between -1.0 and -0.7) and the nanoseismicity induced by the injection. During nearly 5 years of monitoring from November 2009 to July 2014, about two and half thousands of seismic events have been detected, and 628 with magnitude higher than -2.3 have been located in the vicinity of the injection point, within a 500-m radius, allowing for a detailed analysis of reservoir behavior. None of the events had an adverse impact on reservoir integrity. These events are at least 30,000 times less powerful than the lowest threshold of human perception. These were located within the CO_2 plume and along known structural features (induced seismicity). The R&D downhole array removed any ambiguity surrounding injection induced nanoseismicity or caprock integrity [8,9].

Actual network performances are in line with expectations. The effective Master Network "location" sensitivity is better than magnitude -0.5 in the volume of interest (~5-km radius, down to 6-km depth). The addition of a seismometer to the Master Network allows detecting and locating weaker earthquakes than those located by the French National seismological networks. The Research Network allows detecting and locating most nanoseismic events with magnitude higher than -2 within a 500-m zone around the antenna (extension of the CO_2 nanoseismic cloud).

4.2. Results - Spatial distributions of events

After extended work on velocity model calibration, accounting for all available relevant data, the majority of seismic and microseismic events could be located along, or at the vicinity of, known faults mapped thanks to 3D seismic, and the majority, if not all, of nanoseismic events are located within the reservoir in which CO_2 has been injected (Fig. 8). This is an encouraging observation from the perspective of caprock integrity.

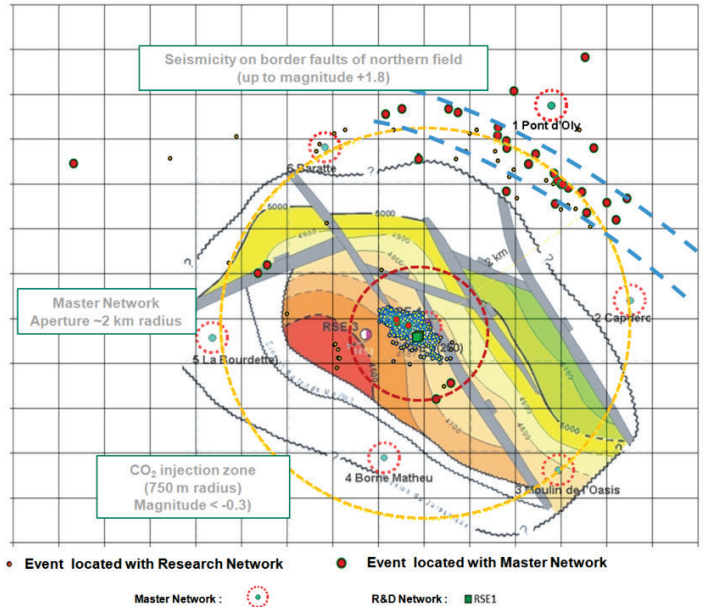

Fig. 8 - Epicenter map of seismic events detected and located by the hybrid network.
In the background, structural sketch map of a horizon not far from reservoir.
Large circles indicate SBA locations. Events are sized by network.
Small dots correspond to nanoseismicity located with Research Network. Larger dots correspond to events located by the Master Network.

4.3. Results - Earthquake reporting (Natural Seismicity)

For public awareness/assurance, regional monitoring of natural seismicity was achieved using a surface seismometer. The Master Network, the combination of the seismometer with the SBAs, allowed detecting and locating smaller earthquakes than the National Network (sensitivity better than 1.5 within a 30-km radius around the injection).

4.4. Results - Seal integrity (Triggered Seismicity)

The SBA-network, a component of the Master Network, has been designed with a focus on seal integrity. One array is by the injector well, and 6 are positioned roughly 2 kilometers around it.

The SBA network "effective location sensitivity" is about magnitude -0.7, in a 2.5-km radius and down to 6-km depth. 71 events (32 by Master Network + 39 by Research Network only - Fig. 8) with magnitude ranging up to 1.8 have been detected and associated to fault type seismicity located on faults mapped with 3D seismic. This type of seismicity was detected before, during and after CO_2 injection and is thought to be related to the past production of a depleted gas field, at the North of Rousse.

The number of events is too small to properly analyze their magnitude frequency distribution and conclude unambiguously about their nature. However, the b-value seems to be more related to planar fault type distribution (b value ~1) and some preliminary focal mechanism analysis performed on a few large-enough events indicates normal faulting or normal strike slip in line with geological and geomechanical analysis.

4.5. Results – Injectivity (Induced seismicity): static analysis of nanoseismicity

628 seismic events have been located with the Research Network, and less than ten with the Master Network.

During 5 years of monitoring, thanks to the Research Network, the downhole vertical array deployed above the injection zone, Thanks to the downhole vertical array deployed above the injection zone, approximately 2560 nanoseismic events were detected, a quarter of them, with magnitude ranging from -2.3 to -0.5, could be located in the vicinity of the injection point.

Key "static" observations are:

- The orientation and the extension of the nanoseismicity cloud are in line with expected CO_2 plume extension and main structural directions.
- The extension of the nanoseismicity cloud is about 500 m.
- The majority of events appear to be located within the reservoir close to the injection point, with trends following identified fault directions (~N150).
- The majority of events have magnitude lower than -1.0 (nanoseismicity).
- The highest magnitude is about -0.5 (still nanoseismicity).
- The magnitude frequency distribution (Fig. 9) has a b-value higher than -2, a characteristic of induced type of seismicity.
- The downhole array network "location sensitivity" is about -2.4 (minimum magnitude for event location) but the magnitude of completeness is about -1.5 (highlighting some viewing bias for events with magnitude smaller than -1.6), in line with our expectations (Fig. 9).

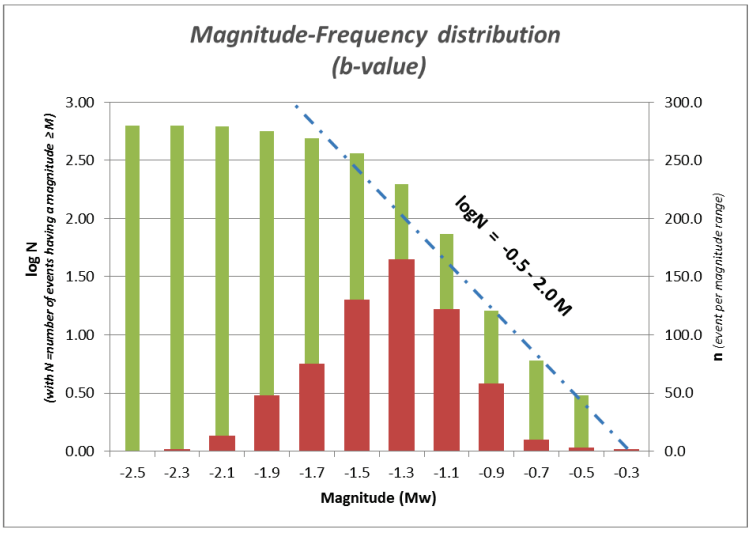

Fig. 9 – Magnitude-frequency distribution histogram (red) and Gutenberg-Richter plot (green) for events located in the CO_2 zone.

4.6. Results - Injectivity (Induced seismicity): dynamic analysis of nanoseismicity

For the dynamic analysis of the (nano)seismicity induced by the CO_2 injection, i.e. its correlation with injection parameters, only located events with a magnitude larger than -1.7 are considered. As the objective is to analyze the evolution of the seismic deformation within the CO_2 zone (radius of 500 m), we need to avoid the bias associated to the viewing distance.

For analysis purposes, the monitoring period has been divided into 4 sub-periods (see Fig. 11): Baseline (before injection start) - First Injection Phases (2010) - Main Injection Phases (2011-2013) - Post Injection Phase (post-2013).

The passive seismic monitoring equipment used during the Baseline Period is the Master Network. The monitoring confirmed the predicted detection sensitivity of the network, with more than 200 natural earthquakes detected and 2 low magnitude local events located along the northern faults.

The First Injection Phase covered a one-year period. During this period, the Master Network recorded natural seismicity, 3 local events on Rousse/Meillon faults and 3 events in the CO2 injection zone (less than 300-m away from injection point).

The Main Injection Phase covers a two-year period. The Master Network kept detecting natural regional seismicity, local seismic events with a magnitude ranging up to 1.8 located in deep structures, and 12 “CO2 zone” events, with a magnitude ranging from -0.9 to -0.5. The Research Network detected about 2500 smaller magnitude events among which 628 were located.

Both the Master Network and the Research Network keep on recording during the ongoing Post Injection Phase. The Master Network has not detected any “CO2 zone” events so far, while the Research Network keeps on recording smaller magnitude events: the nanoseismicity rate remains similar to the one observed during the last months of injection phase.

Key observations:

- The Master Network proved efficient and has not recorded any event above any of the alert thresholds.
- The R&D downhole array calibrated the Master Network performance.
- The Research Network allowed recording sufficient nanoseismicity for detailed analysis of seismicity features.
- During the main injection phase, the seismicity appears to occur always in the same volume (Fig. 10): the space and time distributions of the located events do not present any obvious migration of the seismicity with time. The “seismic deformation” volume seems to remain the same during the whole “main injection” phase.

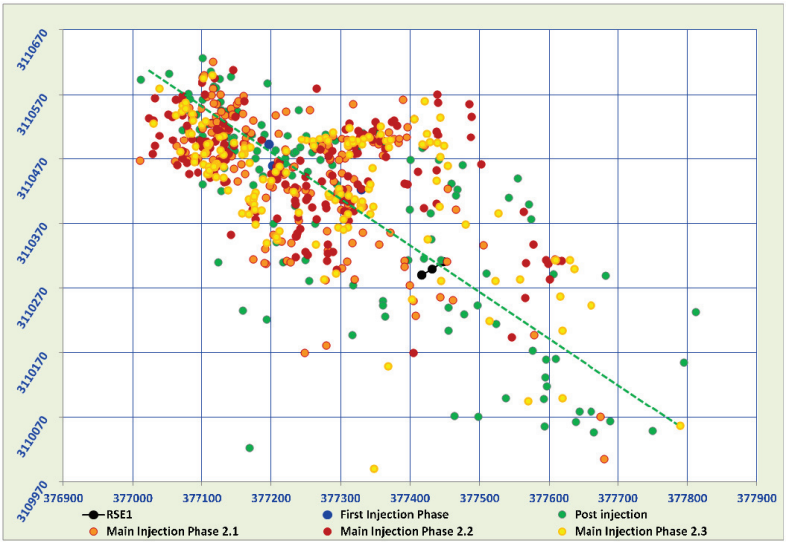

Fig. 10 - Epicenter map of seismic events detected by the Master and Research Networks. Events color coded by time period (see Fig. 11 for definition of time periods)

- Both the cumulative number of events and the cumulative seismic moment seem to correlate with the injection trends described by the cumulative volume of CO_2 (Fig. 11), and by the downhole pressure. The rate of seismicity mimics the average rate of injection, however it is not proportional to the injection rate. The variation of the seismic "power" (daily seismic moment release) with the injection rate is difficult to interpret. A single seismic event releasing the average measured amount of daily energy would have a magnitude between -1.7 to -1.2.

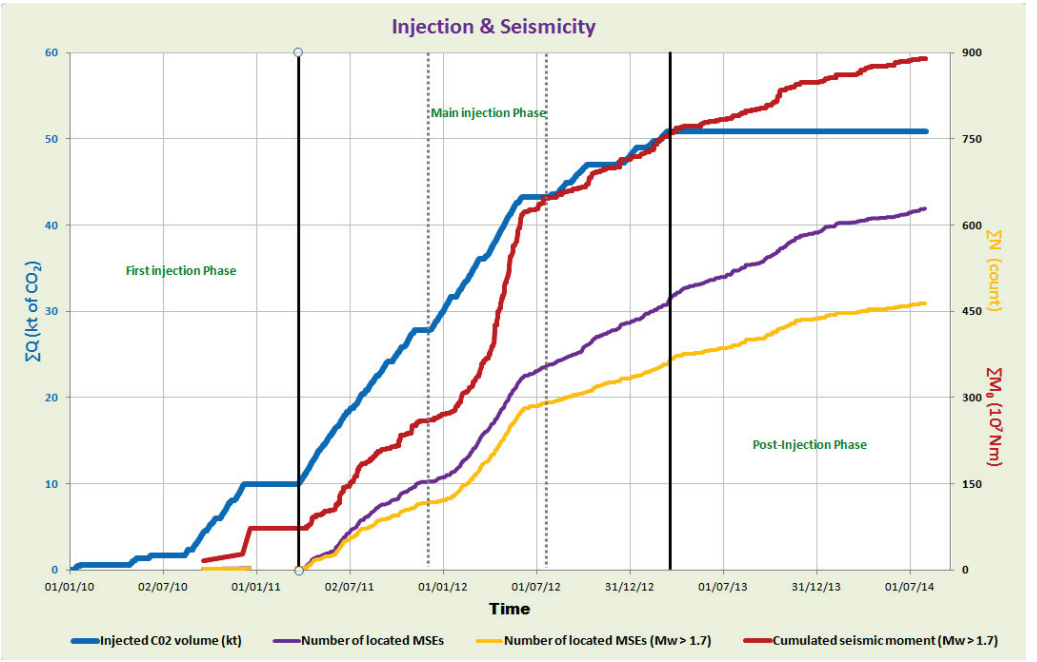

Fig. 11 - Seismicity and injection histories
Cumulative number of located events (purple line), cumulative number of located events with magnitude larger than1.7 (orange line), cumulative seismic moment (red line), and cumulative injected volume of CO_2 (blue line).
Seismicity level trends and injection trend, described by the cumulative injected volume of CO_2, appear to be correlated: the rate of seismicity varies with the average rate of injection.

- As expected, the total effective seismic deformation ($\sum M_{0eff}$) is far below the maximum seismic deformation as per McGarr law ($\sum M_{0McG} = \mu.\Delta V$, i.e. K equals to one). The change in volume resulting from CO_2 injection appears not to be fully accommodated by seismic failure. The cumulative seismic moment (as of 16 months after the end of injection) associated to the total volume of injected fluid leads to a very low "seismic deformation index" Keff < 0.6 10^{-6}. The maximum magnitude of -0.3 (event recorded by the Master Network end 2010) is far below the upper bound predicted by the McGarr law (magnitude +4.7).
- We have also computed $K_{eff}(\Delta t)$ by considering the effective "seismic deformation index" as a function of time and volume injected:

$$K_{eff}(\Delta t) = \sum M_{0eff}(\Delta t) / \mu.\Delta V(\Delta t) = \sum M_{0eff}(\Delta t) / \sum M_{0McG}(\Delta t) \quad (\Delta t = \text{current time - injection start time})$$

The time-varying seismic deformation index follows the average rate of injection. The index seems to indicate an increase of seismicity associated to a nominal injection rate above 110 t/day followed by a steady state rate for the last injection phase (lower nominal rate of 75 t/day) and the post injection phase (Fig. 12).
- The seismic deformation associated to CO_2 injection started almost with the beginning of injection. The index rises during the main injection phase with a strong increase during sub-phase 2 corresponding to the higher injection rate. This suggests that a very small change in volume was able to induce seismicity (locally critical status of stress) and that injection rate is playing a key role in the level of seismicity.

- Seismic deformation did not stop after the injection phase and is still ongoing more than a year after the end of injection. This could suggest that the total change in volume is slowly accommodated by very small seismic deformation (on-going stabilization). Actually another explanation is that additional energy is constantly input into the reservoir. This is supported by reservoir engineering studies that have demonstrated that the Mano reservoir is naturally and constantly refilled by gas from lateral panels, and is still experiencing gas equilibration following the production phase [11]. CO_2 injection has a secondary impact on the measured pressure increase.

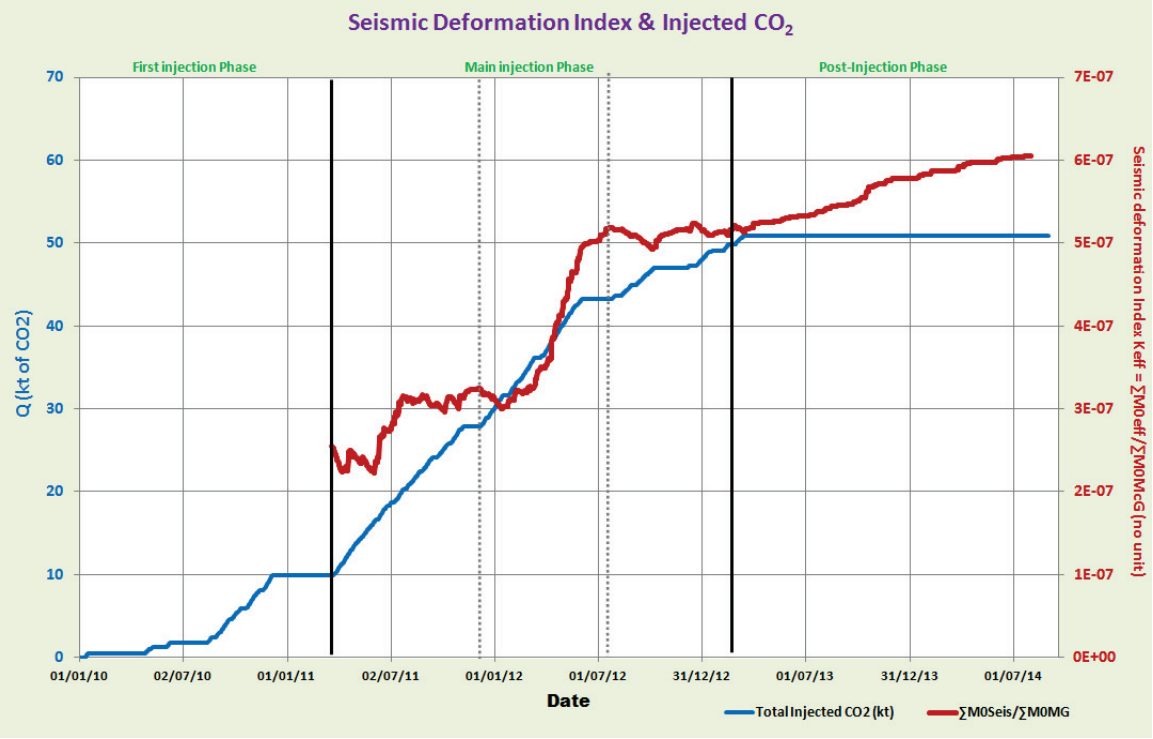

Fig. 12 – Seismic Deformation Index (effective parameter K introduced in the McGarr law - no unit)
$K_{eff}(t) = \sum M_{0eff}(t) \ / \sum M_{0McG}(t)$ (t elapsed time since the beginning of injection)

Key learning:

- The induced nanoseismicity is limited to the modeled CO_2 plume zone and the seismic deformation follows the average rate of injection.
- The largest observed nanoseismic event in the $C0_2$ zone is much smaller than the seismologic potential (M +4.7) as estimated with McGarr equation. Actually, as per mid-2014, the total seismic energy of nanoseismicity recorded within the CO_2 zone corresponds to a single event of magnitude +0.6 (seismic efficiency smaller than one millionth).
- The seismic deformation rate seems to be clearly driven by the volume injected and the rate of injection. However, during a long period of relatively constant injection rate, the seismic deformation rate presents some plateau and rise suggesting a complex relationship possibly including a time delay between cause and effect.
- The Seismic Deformation Index (SDI) appears as a possible indicator to analyze the rate of deformation accommodated by seismic failures within a given volume of rock. The evolution of SDI with time may allow characterizing the trends of seismic activity along with total volume and injection rate. After further analysis, this could be used to mitigate the risk of inducing events felt on surface by adjusting the injection rate.
- For future projects, a longer base line survey than previously planned (at least one year) is advisable to analyze the potential impact of local injection on the reservoir scale.

Final remarks:

- The elements of our study have to be considered acknowledging the fact we are dealing with a complex system that has undergone very large stress changes during depletion with little amount of re-injection compared to the large volume of fluid removed. Intuitively we would expect the re-pressurization process to release some of the stresses in an elastic system, and attenuate potential seismic effects.
- There is an intrinsic difficulty when dealing with a Gutenberg-Richter distribution with b-value larger than 1.5. The methodology applied to assess energy balance needs to be scrutinized as the results are quite sensitive to the network sensitivity and the cut-off magnitude used in the computation.

5. Conclusion

The three-scale network multifocal approach adopted for the passive seismic monitoring of the storage component of the integrated Lacq-Rousse CCS project is perfectly suited. It complies with the requested operational and research objectives for the passive seismic monitoring. It allows recording natural seismicity, seismicity related to the regional context (depleted gas fields) and local nanoseismic events potentially characterizing the small-scale mechanical disturbances induced by CO_2 injection.

The Master Network is roughly performing according to the expectations listed during the feasibility study. The effective location sensitivity is about magnitude -0.6 (completeness magnitude) in the volume of interest (5 km x 5 km x 5 km): any event with a larger magnitude is detected and located by the near-surface network with less than 250-m uncertainty. The expected sensitivity provided by the Master Network is validated thanks to the recording and location of some nanoseismic events with magnitude larger than -1.0, confirming its ability to serve for an efficient seismic hazard monitoring.

The experiment clearly established the proof-of-concept of a seismic hazard monitoring based upon a near-surface monitoring network, in a suburban environment, for gas injection in a reservoir about 5-km deep. As a conclusion, even with a limited number of sensors, a near-surface network is a very effective hazard monitoring tool that can be used as an early warning system, which should be sufficient for most operations.

As expected, the seismicity detected by the Master Network corresponds mainly to natural seismic activity linked to North Pyrenees faults. Only very minor events have been recorded in the reservoir by the Research Network, in the vicinity of the injection points: no events corresponding to any of the considered “Alert Thresholds” have been detected. The additional downhole array deployed for research purposes provides the required sensitivity to record locate and analyze induced nanoseismicity within the reservoir. This allows confirming without any ambiguity that in the specific context of the project, injection has no incidence on caprock integrity, in full agreement with the geomechanical studies.

Finally, in first approximation, the experiment also allows analyzing the relationship between induced-seismic deformation (moment) and the volume injected. The McGarr equation law has been used to assess both the maximum potential seismic deformation (upper bound) and the effective seismic deformation rate. The seismic deformation index inferred from this approach raises expectations that such an analysis could provide a powerful continuous risk evaluation tool, through permanent comparison between observed nanoseismic activity with the fluid volume input into, or output out of, the reservoir. This second type of application is certainly not necessary for most developments, but it can constitute a precise element of monitoring.

Reservoir studies indicate that observed nanoseismicity might also be connected to the ongoing gas reequilibration following the large production period, when pressure was decreased from 485 to 42 bars.

Obviously a downhole array provides a lot of information for managing strong or unknown seismic hazards. Nevertheless we are fully confident that in most situations, a properly designed surface or near-subsurface network would provide the required sensitivity to collect the data necessary for verifying that operations are taking place safely and as anticipated.

Acknowledgments

The authors wish to acknowledge Total Exploration Production for permission to publish this work.

References

[1] Gapillou C, Thibeau S, Mouronval G and Lescanne M. Building a geocellular model of the sedimentary column at Rousse CO_2 geological storage site (Aquitaine, France) as a tool to evaluate a theoretical maximum injection pressure. Energy Procedia 2009; 1, 2937–2944

[2] Arrété Préfectoral 09/IC/122. http://www.pyrenees-atlantiques.gouv.fr/content/download/7583/47194/file/AP2009-05-13.pdf (in French)

[3] Prinet C, Thibeau S, Lescanne M, Monne J. Lacq-Rousse CO_2 Capture and Storage demonstration pilot: Lessons learnt from two and a half years monitoring. Energy Procedia 2013; 37, 3610 – 3620

[4] Ellsworth WL. Injection-Induced Earthquakes. Science 2013; 341.

[5] Bohnhoff M, et YIG. From Microseismicity to Large Earthquakes: Studies Related to Seismic Hazard Assessment, Carbon Sequestration and Sustainable Resource Management. ILP Second Potsdam Conference, 6-8 Oct. 2010

[6] Dahm T, Hainzl S, Becker D, and the FKPE group DINSeis. How to discriminate induced, triggered and natural seismicity. Proceedings of the Workshop Induced seismicity: November 15 - 17, 2010, Hotel Hilton, Luxembourg.

[7] Zoback MD, and Gorelick SM. Earthquake triggering and large-scale geologic storage of carbon dioxide. Proceedings of the National Academy of Sciences of the United States of America 2012; 109, 26, 10164-10168

[8] McGarr A. Seismic Moments and Volume Changes. Journal of Geophysical Research 1976; 81, 8, 1487–1494.

[9] McGarr A. Maximum magnitude earthquakes induced by fluid injection. Journal of Geophysical Research 2004; 119, 2, 1008–1019.

[10] Pourtoy D, Onaisi A, Lescanne M, Thibeau S, Viaud C. Seal Integrity of the Rousse depleted gas field impacted by CO_2 injection (Lacq industrial CCS reference project France). Energy Procedia 2013; 37, 5480 – 5493

[11] Thibeau S, Chiquet P, Prinet C, Lescanne M. Lacq-Rousse CO2 Capture and Storage demonstration pilot: Lessons learnt from reservoir modelling studies. Energy Procedia 2013; 37, 6306– 6316